Robust Fault Reconstruction for LPV Systems Using Sliding Mode Observers

Halim Alwi and Christopher Edwards

Abstract

This paper presents a robust FDI scheme using a sliding mode observer based on an LPV system, with fault reconstruction capability. Both actuator and sensor fault reconstruction schemes are considered which possess robustness against a certain class of uncertainty and corrupted measurements. For actuator fault reconstruction, the input distribution matrix (associated with the actuators being monitored) is factorized into fixed and varying components. LMIs are used to design the key observer parameters in order to minimize the effect of uncertainty and measurement corruption on the fault reconstruction signal. The faults are reconstructed using the output error injection signal associated with the nonlinear term of the sliding mode observer. For sensor fault reconstruction, the idea is to re-formulate the problem into an actuator fault reconstruction scenario so that the same design procedure can be applied. This is achieved by augmenting the original system with the filtered sensors being monitored. Simulations using a full nonlinear model of a large transport aircraft are presented, and show good fault reconstruction performance.

I. Introduction

Fault detection and isolation (FDI) is an important feature, for timely detection of faults. It provides awareness to the operator of any faults present in the system and allows appropriate action to be taken quickly. Also, in active fault tolerant control [40], fast FDI is crucial in providing fast controller reconfiguration to attempt to maintain the level of performance.

FDI using linear based observers is a mature field of study. For practical implementation, one of the challenges of linear observer design is to ensure performance over wide operating conditions. Linear FDI designs usually perform well close to the design point, but the performance might degrade as the system moves away. This may lead to poor fault detection performance, and result in false alarms or missed detection. To overcome this issue, a popular and widely used method in industry, especially in aerospace applications, is to use gain scheduling. However, typically these schemes are based on ad-hoc methods. Although it is a convenient form of scheduling (where the gains designed at multiple trim points are scheduled), as argued in [8], these ad-hoc methods lack proofs and guarantees of performance and even stability (other than at the designed points). Furthermore, from a practical point of view, having to implement families of observers designed about many points to cover a wide range of operating conditions is both time consuming to design, and can be complicated to implement. A more formal way to extend linear time invariant (LTI) based designs is to consider a Linear Parameter Varying (LPV) approach. In LPV based designs the gains are automatically scheduled during the design process through the plant varying parameters. There has been significant research in these areas in the last decade in order to exploit the convenience of extending LTI design methods to achieve performance and stability guarantees. A significant portion of this research has been directed towards FDI (see for examples [7], [9], [10], [11], [21], [22], [34], [41], [37]).

One obvious benefit of LPV based design is the formal stability proofs and guarantees of robustness over a wide set of operating conditions. The applicability of the underlying linear design strategies with extension to LPV systems, means there is no requirement for a total redevelopment of new FDI design. The simplicity and the convenience of exploiting already widely used linear design methodologies means conversion into an LPV framework allows simpler transition when applied to the actual system. Although there are direct nonlinear model based FDI approaches for nonlinear systems (see for example [5], [12], [1]), most of them require radically new FDI design approaches. However in aircraft systems and other safety critical application, this leads to implementation and certification issues.

H. Alwi and C. Edwards are currently with the College of Engineering, Mathematics and Physical Sciences, University of Exeter, EX4 4QF, UK. h.alwi@exeter.ac.uk, C.Edwards@exeter.ac.uk

In some cases it is much easier and more convenient to use an LPV based design due to model availability. For example, in aircraft systems, a nonlinear FDI observer design often requires information about the aerodynamic coefficients, which is hard to obtain in the required form. However an LPV representation can easily be built from available families of linear systems over the entire flight envelope (see [8], [29] for examples of LPV system development and [32] for a recent generalized LPV model generation scheme). Through polynomial fitting, the LPV models may explicitly contain information about the aerodynamic coefficient variations over the flight envelope. This is convenient and readily available information, which can be used to retain a good fidelity level compared to the actual system. Therefore LPV based design seems to provide a good compromise between local LTI methods and a full blown nonlinear design.

For practical implementation of FDI schemes, robustness issues with regard to plant model-mismatch, uncertainty and sensor measurement corruption have to be taken into consideration. Despite the potential benefit of employing an LPV based design, the LPV model used as the basis of the observer will be imperfect, and this might cause false alarms or missed detections. For a LPV model generated using an interpolation of families of localized linear models (which is a commonly used approach), plant-model mismatch is present (especially) in the interpolated region where the model is not well defined (see for example [25], [29] for validation tests of an LPV plant comparing the actual plant states and LPV states). Other LPV generating methods will contain imperfect plant information due to simplifications and assumptions. Therefore robustness issues have to be considered during the FDI design process in order to minimize the risk of missed detections or false alarms. This motivates the work which will be presented in this paper.

Another emerging technique in the field of FDI is the sliding mode approach. The early work (see for example [24], [43]) uses traditional residual ideas for the output estimation error in order to detect faults. In [24], [43] the sliding motion is allowed to break in the presence of faults/failures in the system. More recent work [44], [26] and especially [14], [38], [16] uses the robustness property of sliding modes to provide not only the detection of faults, but also more information about the 'size' and 'shape' of the faults. This is achieved through reconstruction of the faults by analyzing the 'output error injection' signals which are required to maintain sliding even in the presence of faults. In systems where redundancy is not available, the reconstruction of faults can be beneficial – especially for sensor fault tolerant control problems (see for example [2]). However, most of the work in this area is developed based on LTI or quasi linear systems (see for example [42]) and is therefore restricted to near trim conditions.

There has been relatively little previous work in the area of sliding modes applied to LPV systems. That said, notable exceptions in the area of control are described in [36], [31]), and recent work [15] has applied higher order sliding mode ideas to LPV systems for so-called interval observers. Recently, the work in [3] explored the potential of using sliding mode techniques for LPV systems, specifically for FDI with fault reconstruction. The design in [3] employs a simple pole placement method to exploit the design freedom but does not consider uncertainty in the system or measurement disturbances. In this paper, a more advanced design approach compared to [3] will be considered, and a Linear Matrix Inequality (LMI) synthesis approach will be applied to ensure robustness. Similar to the LTI based design proposed in [38], the idea is to minimize the effect of uncertainty and sensor measurement corruption on the quality of the fault reconstruction signals.

This paper proposes a fault reconstruction scheme based on a LPV system representation for both actuator and sensor faults which is robust against sensor measurement corruption and a certain class of model uncertainty.

The observer is designed using a 'virtual' system associated with the fixed distribution matrix and the other system matrices. The observer gains comprise varying linear and fixed nonlinear components (associated with the nonlinear term). The 'virtual fault' is reconstructed through appropriate scaling of the equivalent output error injection signal, and this is mapped back to actual actuator faults by rearranging the factorized input distribution matrix. For sensor faults, the idea is to re-formulate the problem into an actuator fault reconstruction scenario so that the same design procedure can be used. This problem re-formulation is achieved by augmenting the original system with filtered versions of the sensors being monitored. This augmentation is of lower order compared to the one proposed in [38], where the original system is augmented with the filtered version of all the outputs. This is advantageous as a much lower (augmented) system order will be considered in the LMI analysis during the observer design. Second order sliding mode methods (which require no smoothing) will be considered for the equivalent output error injection signal. This scheme still allows an ideal sliding motion to be achieved (without any smoothing) and therefore preserves the robustness property of sliding modes.

Simulation results from an established nonlinear aircraft benchmark model (associated with the European FP7 'Advanced Fault Diagnosis for Sustainable Flight Guidance and Control' (ADDSAFE) project[1]) will be used to demonstrate the proposed scheme for reconstructing a sensor fault. This constitutes one of the benchmark problems which is being investigated in the ADDSAFE project.

The notation employed is reasonably standard. The expression I_n represents an identity matrix of order n, the symbol $\mathbb{R}$ represents the field of real numbers and $\mathcal{R}(\cdot)$ represents the range space of the matrix. Finally $\|\cdot\|$ represents the Euclidean norm of vectors or the induced spectral norm for matrices.

II. LPV SYSTEM DESCRIPTION

Consider an uncertain (affine) LPV plant subject to actuator faults represented by

$$\dot{x}(t) = A(\rho)x(t) + B(\rho)u(t) + H(\rho)f_i(t) + M\xi(t,y,u) \quad (1)$$

$$y(t) = Cx(t) + d(t) \quad (2)$$

where $A(\rho) \in \mathbb{R}^{n\times n}, B(\rho) \in \mathbb{R}^{n\times m}, H(\rho) \in \mathbb{R}^{n\times q}$ are parameter varying matrices, while $C \in \mathbb{R}^{p\times n}$ and $M \in \mathbb{R}^{n\times k}$ are fixed matrices. It is assumed that C has full row rank. It is assumed $n > p \geq q$ and that the inputs $u(t)$ and the output measurements $y(t)$ are available for the FDI scheme. The signal $d(t) \in \mathbb{R}^p$ represents a corruption of the true outputs and results in imperfect sensor measurements.

The unknown signal $f_i(t) : \mathbb{R}_+ \to \mathbb{R}^q$ and represents the effect of the actuator faults: when $f_i \neq 0$ a fault exists in the system, and $f_i \equiv 0$ represents nominal fault–free conditions. The signals $\xi(t,y,u) : \mathbb{R}_+ \times \mathbb{R}^p \times \mathbb{R}^m \to \mathbb{R}^k$ encapsulate the uncertainty in the system. It is assumed that $\xi(\cdot)$ is unknown but has a bounded derivative, and $\|\dot{\xi}(t,y,u)\| < b$ where the scalar b is known. The varying parameters, $\rho \in \Omega \subset \mathbb{R}^r$ (where Ω is a compact set), are assumed to be available and perfectly measurable.

Assumption 1: The signal $d(t)$ is low frequency in nature so that from a frequency domain perspective

$$d(s) = G_d(s)\phi(s) \quad (3)$$

for some stable low pass transfer function matrix $G_d(s)$ and unknown input $\phi(s) : \mathbb{R}_+ \mapsto \mathbb{R}^p$. In this paper the simplest possible filter structure is considered given by

$$\dot{d}(t) = -a_f d(t) + a_f \phi(t) \quad (4)$$

where $a_f \in \mathbb{R}_+$ is a positive scalar. This is equivalent to $G_d(s) = \text{diag}(\frac{a_f}{s+a_f}, \ldots, \frac{a_f}{s+a_f})$. In (4), the unknown signal $\phi(t)$ is assumed to be bounded by $\|\phi\| < b_\phi$ where b_ϕ is a positive scalar.

Assumption 2: It will be assumed that $\mathcal{R}(H(\rho)) \subset \mathcal{R}(B(\rho))$ and that the varying matrix $H(\rho)$ can be perfectly factorized into

$$H(\rho) = FE(\rho) \quad (5)$$

where $F \in \mathbb{R}^{n\times q}$ is fixed, and $E(\rho) \in \mathbb{R}^{q\times q}$ is a varying matrix which is assumed to be invertible for all $\rho \in \Omega$. The assumption that $E(\rho)$ is invertible will assist in the reconstruction of the faults, and will be discussed later in the paper.

This factorization is quite common for over actuated systems or for fault tolerant systems with built–in redundancy e.g. large civil aircraft [28]. Using (5), the system in (1) can be rewritten as

$$\dot{x}(t) = A(\rho)x(t) + B(\rho)u(t) + F\underbrace{E(\rho)f_i(t)}_{f_\nu(t,\rho)} + M\xi(t,y,u) \quad (6)$$

where the signal $f_\nu(t,\rho) : \mathbb{R}_+ \times \mathbb{R}^r \to \mathbb{R}^q$ represents the unknown 'virtual faults'. The observer design strategy will initially estimate $f_\nu(t,\rho)$ instead of $f_i(t)$. The estimation of the actual fault $f_i(t)$ can then be derived from the estimates of $f_\nu(t,\rho)$. Assume that

$$\|f_\nu(t,\rho)\| < a(t,\rho,u) \quad (7)$$

where $a(t,\rho,u) : \mathbb{R}_+ \times \mathbb{R}^r \times \mathbb{R}^m \to \mathbb{R}_+$ is a known bounded function.

[1] http://addsafe.deimos-space.com

III. LPV SLIDING MODE OBSERVER

A. Observer Structure

The proposed observer has the structure

$$\dot{\hat{x}}(t) = A(\rho)\hat{x}(t) + B(\rho)u(t) - G_l(\rho)e_y(t) + G_n\nu(t) \tag{8}$$

$$\hat{y}(t) = C\hat{x}(t) \tag{9}$$

where $G_l(\rho), G_n \in \mathbb{R}^{n\times p}$ are the observer gain matrices and $\nu(t)$ represents a nonlinear function of the output estimation error to induce a sliding motion [14] (which will be discussed later). The output estimation error

$$e_y(t) := \hat{y}(t) - y(t) = Ce(t) - d(t) \tag{10}$$

where $e(t) = \hat{x}(t) - x(t)$. Subtracting (6) from (8) yields the state estimation error system

$$\dot{e}(t) = A(\rho)e(t) - G_l(\rho)e_y(t) + G_n\nu(t) - Ff_\nu(t) - M\xi(t) \tag{11}$$

The objective is to force the output estimation error $e_y(t)$ to zero in finite time, and induce a sliding mode on the sliding surface

$$\mathcal{S} = \{e(t) \in \mathbb{R}^n : e_y(t) = 0\} \tag{12}$$

In the ideal case when the measurement corruption term $d(t) = 0$, $\mathcal{S}$ in (12) corresponds to a surface on which the output of the observer exactly follows the plant output. The idea is that, during sliding, the signal $f_\nu(t,\rho)$ will be estimated using the 'equivalent output injection' [13], [14], [38] (i.e. the signal $\nu(t)$ must take on average to maintain sliding). The design freedom associated with the observer in (8) are the design gains $G_l(\rho)$ and G_n. In sliding mode observers, it is the gain associated with the nonlinear injection terms which is important (in this case G_n), since during sliding $e_y = 0$, and the effect of $G_l(\rho)$ is diminished. However, the choice of $G_l(\rho)$ can be exploited to ensure global state estimation error convergence.

Assumption 3: $\text{rank}(CF) = q$

Since F in (5) is a fixed matrix and CF is full rank, there exists a coordinate transformation $x(t) \mapsto T_o x(t)$ (where $T_o \in \mathbb{R}^{n\times n}$), similar to the one proposed in [14], which gives a coordinate system in which the output distribution matrix has the structure

$$y(t) = \underbrace{\begin{bmatrix} 0 & T \end{bmatrix}}_{C} \begin{bmatrix} x_1(t) \\ x_2(t) \end{bmatrix} + d(t) \tag{13}$$

where $T \in \mathbb{R}^{p\times p}$ is orthogonal, and the fault distribution matrix

$$F = \begin{bmatrix} \frac{0_{(n-p)\times q}}{F_2} \end{bmatrix} = \begin{bmatrix} \frac{0_{(n-p)\times q}}{0} \\ F_o \end{bmatrix} \tag{14}$$

where $F_2 \in \mathbb{R}^{p\times q}$ and $F_o \in \mathbb{R}^{q\times q}$ and is nonsingular. In these coordinates the system matrix $A(\rho)$ is not assumed to have any special structure. At this juncture, no special structure will be imposed on $G_l(\rho)$ from (8), but it will be assumed

$$G_n = \begin{bmatrix} -LT^{\mathrm{T}} \\ T^{\mathrm{T}} \end{bmatrix} \tag{15}$$

where the design matrix $L \in \mathbb{R}^{(n-p)\times p}$ is assumed to have a special structure

$$L = \begin{bmatrix} L_1 & 0 \end{bmatrix} \tag{16}$$

with $L_1 \in \mathbb{R}^{(n-p)\times(p-q)}$. Whilst (15) appears to have a restricted structure, it is shown in earlier work ([14]) that L_1 is in fact a parametrization of the available freedom to influence the reduced order sliding motion. In this observer regular form, the error system (11) can be written in detail as

$$\begin{bmatrix} \dot{e}_1(t) \\ \dot{e}_2(t) \end{bmatrix} = \underbrace{\begin{bmatrix} A_{11}(\rho) & A_{12}(\rho) \\ A_{21}(\rho) & A_{22}(\rho) \end{bmatrix}}_{A(\rho)} \begin{bmatrix} e_1(t) \\ e_2(t) \end{bmatrix} - \underbrace{\begin{bmatrix} 0 \\ F_2 \end{bmatrix}}_{F} f_\nu(t,\rho) - \underbrace{\begin{bmatrix} M_1 \\ M_2 \end{bmatrix}}_{M} \xi - \underbrace{\begin{bmatrix} G_{l_1}(\rho) \\ G_{l_2}(\rho) \end{bmatrix}}_{G_l(\rho)} e_y(t) + \underbrace{\begin{bmatrix} -LT^{\mathrm{T}} \\ T^{\mathrm{T}} \end{bmatrix}}_{G_n} \nu(t) \tag{17}$$

where $e_1(t) \in \mathbb{R}^{n-p}$ and $e_2(t) \in \mathbb{R}^p$. The gain sub–matrices $G_{l_1}(\rho) \in \mathbb{R}^{(n-p)\times p}$, $G_{l_2}(\rho) \in \mathbb{R}^{p\times p}$. The objective is to design the matrix L (in the definition of G_n) in (15) since this matrix affects the sliding motion dynamics. A design methodology for L and G_l for LTI systems appears in [38]. This paper will propose a different strategy for designing L and $G_l(\rho)$ based on the problem formulation discussed earlier.

B. Observer Design

Notice from (13) and (10) that

$$e_y(t) = Te_2(t) - d(t) \tag{18}$$

During an ideal sliding motion, $\dot{e}_y(t) = e_y(t) = 0$, therefore from (18), $Te_2(t) = d(t)$ and $T\dot{e}_2(t) = \dot{d}(t)$. During sliding, substituting for these quantities in (17) yields

$$\begin{aligned} \dot{e}_1(t) &= A_{11}(\rho)e_1(t) + A_{12}(\rho)T^{\mathrm{T}}d(t) - LT^{\mathrm{T}}\nu_{eq}(t) - M_1\xi(t) & (19)\\ 0 &= TA_{21}(\rho)e_1(t) + TA_{22}(\rho)T^{\mathrm{T}}d(t) + \nu_{eq}(t) - TF_2f_\nu(t) - TM_2\xi(t) - \dot{d}(t) & (20) \end{aligned}$$

where the signal $\nu_{eq}(t)$ is the so-called 'equivalent output injection' signal [14] which is required to maintain a sliding motion. Let $\hat{d}(t) := T^{\mathrm{T}}d(\mathrm{t})$ and solve for $\nu_{eq}(t)$ from equation (20) to give

$$\nu_{eq}(t) = -TA_{21}(\rho)e_1(t) - TA_{22}(\rho)\hat{d}(t) + TF_2f_\nu(t) + TM_2\xi(t) + \dot{d}(t) \tag{21}$$

Substituting (21) into (19) and using the fact that $LF_2 = 0$ and $\dot{\hat{d}}(t) = T^{\mathrm{T}}\dot{d}(t)$ yields

$$\dot{e}_1(t) = (A_{11}(\rho) + LA_{21}(\rho))e_1(t) + (A_{12}(\rho) + LA_{22}(\rho))\hat{d}(t) - (M_1 + LM_2)\xi(t) - L\dot{\hat{d}}(t) \tag{22}$$

Define a reconstruction signal as

$$\hat{f}_\nu(t) = WT^{\mathrm{T}}\nu_{eq}(t) \tag{23}$$

where W has a structure

$$W = \begin{bmatrix} W_1 & F_o^{-1} \end{bmatrix} \tag{24}$$

and $W_1 \in \mathbb{R}^{q\times(p-q)}$ is design freedom. The square invertible matrix F_o is from (14), and thus W has only partial design freedom. Multiplying (21) with WT^{T} and rearranging yields

$$\hat{f}_\nu(t) - f_\nu(t) = -WA_{21}(\rho)e_1(t) - WA_{22}(\rho)\hat{d}(t) + WM_2\xi(t) + W\dot{\hat{d}}(t) \tag{25}$$

since $WF_2 = I_p$ for any choice of W_1.

Substituting (4) into (22) and (25) and augmenting $e_1(t)$ with $d(t)$ to create $e_a(t) = \mathrm{col}(\hat{d}(t), e_1(t))$, yields the system

$$\begin{aligned} \dot{e}_a(t) &= A_a(\rho)e_a(t) + B_a\xi_a(t) & (26)\\ \hat{f}_\nu(t) - f_\nu(t) &= C_ae_a(t) + F_a\xi_a(t) & (27) \end{aligned}$$

where the augmented disturbance signals $\xi_a(t) = \mathrm{col}(\xi(t), \hat{\phi}(t))$ and $\hat{\phi}(t) := T^{\mathrm{T}}\phi(t)$. It follows from (4) that

$$\dot{\hat{d}}(t) = -a_f\hat{d}(t) + a_f\hat{\phi}(t) \tag{28}$$

and the state space matrices from (26)-(27) are given by

$$A_a(\rho) = \left[\begin{array}{c|c} -a_f I_p & 0 \\ \hline A_{12}(\rho) + LA_{22}(\rho) + a_f L & A_{11}(\rho) + LA_{21}(\rho) \end{array}\right] \tag{29}$$

$$B_a = \left[\begin{array}{c|c} 0 & a_f I_p \\ \hline -(M_1 + LM_2) & -a_f L \end{array}\right] \tag{30}$$

$$C_a(\rho) = \left[\begin{array}{c|c} -WA_{22}(\rho) - a_f W & -WA_{21}(\rho) \end{array}\right] \tag{31}$$

$$F_a = \left[\begin{array}{c|c} WM_2 & a_f W \end{array}\right] \tag{32}$$

To introduce extra degrees of design freedom, define a weighting matrix

$$\Delta = diag(\delta_1 I_k, \delta_2 I_p) \tag{33}$$

to scale B_a and F_a in (30) and (32). This extra freedom will be used to introduce a design penalty, trading-off performance against uncertainty in the plant $\xi(t, y, u)$ and corruption to the measurements from $\hat{\phi}(t)$.

The objective now is to design L in (29) and (30) with the structure in (16), which stabilizes $A_{11}(\rho) + LA_{21}(\rho)$ while minimizing the effect of $\xi_a(t)$ on the reconstruction error $\hat{f}_\nu(t) - f_\nu(t)$ in (26) and (27). Using the Bounded Real Lemma [17], if there exist symmetric matrices $P_{a_f} \in \mathbb{R}^{p\times p}$ and $P_{11} \in \mathbb{R}^{(n-p)\times(n-p)}$ such that

$$\left[\begin{array}{ccc} A_a^{\mathrm{T}}(\rho)P_1 + P_1 A_a(\rho) & P_1(B_a\Delta) & C_a^{\mathrm{T}} \\ (B_a\Delta)^{\mathrm{T}}P_1 & -\gamma I & (F_a\Delta)^{\mathrm{T}} \\ C_a & (F_a\Delta) & -\gamma I \end{array}\right] < 0 \tag{34}$$

$$P_1 = \left[\begin{array}{cc} P_{a_f} & 0 \\ 0 & P_{11} \end{array}\right] > 0 \tag{35}$$

then $\|\hat{f}_\nu - f_\nu\| < \gamma\|\xi_a\|$. Note that the structure of P_1 in (35) introduces conservatism but will be shown to aid tractability.

Using arguments similar to those in [41], it will be assumed that the system in (26) and (27) can be represented as a polytopic system where the range of admissible ρ corresponds to a polytope $\mathcal{R}$ with vertices $\omega_1, \omega_2, \ldots \omega_{n_\omega}$ where $n_\omega = 2^r$. Therefore using the vertex property discussed in [41], [6], the affine LPV system matrices $(A_a(\rho), B_a, C_a(\rho), F_a)$ in (34) and (35) can be replaced by $(A_a(\omega_i), B_a, C_a(\omega_i), F_a)$ and the LMIs in (34) can be solved for all the vertices of the polytopic system.

Once the gain L has been synthesized, apply a further state transformation to the system in (13)-(17) of the form

$$\left[\begin{array}{c} \tilde{e}_1(t) \\ \tilde{e}_2(t) \end{array}\right] := T_L \left[\begin{array}{c} e_1(t) \\ e_2(t) \end{array}\right] \tag{36}$$

where $T_L \in \mathbb{R}^{n\times n}$ is given by

$$T_L := \left[\begin{array}{cc} I & L \\ 0 & T \end{array}\right] \tag{37}$$

and L (defined in (16)) is the design matrix obtained from solving the LMIs associated with (34) and (35).

In the new coordinates the error system from (17) can be written as

$$\begin{bmatrix} \dot{\tilde{e}}_1(t) \\ \dot{\tilde{e}}_2(t) \end{bmatrix} = \underbrace{\begin{bmatrix} \tilde{A}_{11}(\rho) & \tilde{A}_{12}(\rho) \\ \tilde{A}_{21}(\rho) & \tilde{A}_{22}(\rho) \end{bmatrix}}_{\tilde{A}(\rho)=T_L A(\rho) T_L^{-1}} \begin{bmatrix} \tilde{e}_1(t) \\ \tilde{e}_2(t) \end{bmatrix} - \underbrace{\begin{bmatrix} 0 \\ \tilde{F}_2 \end{bmatrix}}_{\tilde{F}=T_L F} f_\nu(t,\rho) - \underbrace{\begin{bmatrix} \tilde{M}_1 \\ \tilde{M}_2 \end{bmatrix}}_{\tilde{M}=T_L M} \xi(t) - \underbrace{\begin{bmatrix} \tilde{G}_{l_1}(\rho) \\ \tilde{G}_{l_2}(\rho) \end{bmatrix}}_{\tilde{G}_l(\rho)=T_L G_l} e_y(t) + \underbrace{\begin{bmatrix} 0 \\ I \end{bmatrix}}_{\tilde{G}_n=T_L G_n} \nu(t) \tag{38}$$

where the fact that $LF_2 = 0$ (because of the structures of F and L in (14) and (16)) has been used to obtain the expression for $\tilde{F}$. The matrix $\tilde{A}(\rho)$ is given as

$$\tilde{A}(\rho) = \left[\begin{array}{cc} \tilde{A}_{11}(\rho) & \tilde{A}_{12}(\rho) \\ \tilde{A}_{21}(\rho) & \tilde{A}_{22}(\rho) \end{array}\right] = \left[\begin{array}{cc} A_{11}(\rho) + LA_{21}(\rho) & A_{12}(\rho)T^T + LA_{22}(\rho)T^T - \tilde{A}_{11}(\rho)T^T L \\ TA_{21}(\rho) & TA_{22}(\rho)T^T - TA_{21}(\rho)T^T L \end{array}\right]$$

By definition, $\tilde{F}_2 = TF_2$ and

$$\tilde{C} = CT_L^{-1} = \left[\begin{array}{cc} 0 & I \end{array}\right] \tag{39}$$

Due to the special structure of L from (16), further partition $A_{21}(\rho)$ from (17) as

$$A_{21}(\rho) = \left[\begin{array}{c} A_{211}(\rho) \\ A_{212}(\rho) \end{array}\right] \tag{40}$$

where $A_{211}(\rho)$ represents the top $(p-q)$ rows of $A_{21}(\rho)$. Then, $\tilde{A}_{11}(\rho)$ from (38) can be written as

$$\tilde{A}_{11}(\rho) = A_{11}(\rho) + L_1 A_{211}(\rho) \tag{41}$$

By construction, if the LMI in (34) is satisfied, L (and L_1) have been designed such that $\tilde{A}_{11}(\rho)$ is quadratically stable. This follows because

$$\tilde{A}_{11}(\rho)^{\mathrm{T}} P_{11} + P_{11}\tilde{A}_{11}(\rho) < 0 \tag{42}$$

for all $\rho \in \Omega$ since the expression in (42) represents the top left sub-block of $A_a(\rho)^{\mathrm{T}} P_1 + P_1 A_a(\rho) < 0$ exploiting the block diagonal form of P_1 in (35). From (10) and (39), $e_y(t) = \tilde{e}_2(t) - d(t)$, and the set of equations from (38) and (4) yield an augmented system

$$\underbrace{\left[\begin{array}{c} \dot{d} \\ \hline \dot{\tilde{e}}_1 \\ \hline \dot{e}_y \end{array}\right]}_{\dot{e}_a(t)} = \underbrace{\left[\begin{array}{cc|c} -a_f I_p & 0 & 0 \\ \tilde{A}_{12}(\rho) & \tilde{A}_{11}(\rho) & \tilde{A}_{12}(\rho) \\ \hline \tilde{A}_{22}(\rho) + a_f & \tilde{A}_{21}(\rho) & \tilde{A}_{22}(\rho) \end{array}\right]}_{\tilde{A}_a(\rho)} \underbrace{\left[\begin{array}{c} d \\ \hline \tilde{e}_1 \\ \hline e_y \end{array}\right]}_{e_a(t)} - \underbrace{\left[\begin{array}{c} 0 \\ \hline 0 \\ \hline \tilde{F}_2 \end{array}\right]}_{\tilde{F}_a} f_\nu(t,\rho) + \underbrace{\left[\begin{array}{c|c} 0 & a_f T \\ \hline -\tilde{M}_1 & 0 \\ \hline -\tilde{M}_2 & -a_f T \end{array}\right]}_{\tilde{M}_a} \xi_a(t) - \underbrace{\left[\begin{array}{c} 0 \\ \hline \tilde{G}_{l_1} \\ \hline \tilde{G}_{l_2} \end{array}\right]}_{G_{l_a}(\rho)} e_y(t) + \underbrace{\left[\begin{array}{c} 0 \\ \hline 0 \\ \hline I_p \end{array}\right]}_{\tilde{G}_{n_a}} \nu(t) \tag{43}$$

Define

$$\left[\begin{array}{c|c} \tilde{A}_{a_{11}}(\rho) & \tilde{A}_{a_{12}}(\rho) \\ \hline \tilde{A}_{a_{21}}(\rho) & \tilde{A}_{22}(\rho) \end{array}\right] := \left[\begin{array}{cc|c} -a_f I_p & 0 & 0 \\ \tilde{A}_{12}(\rho) & \tilde{A}_{11}(\rho) & \tilde{A}_{12}(\rho) \\ \hline \tilde{A}_{22}(\rho) + a_f I_p & \tilde{A}_{21}(\rho) & \tilde{A}_{22}(\rho) \end{array}\right] \tag{44}$$

and

$$\left[\begin{array}{c} \tilde{M}_{a_1} \\ \hline \tilde{M}_{a_2} \end{array}\right] := \left[\begin{array}{cc} 0 & a_f T \\ -\tilde{M}_1 & 0 \\ \hline -\tilde{M}_2 & -a_f T \end{array}\right] \tag{45}$$

Consider a choice of observer gain $\tilde{G}_l(\rho)$ of the form

$$\tilde{G}_l(\rho) := \left[\begin{array}{c} \tilde{G}_{l_1}(\rho) \\ \tilde{G}_{l_2}(\rho) \end{array}\right] := \left[\begin{array}{c} \tilde{A}_{12}(\rho) \\ \tilde{A}_{22}(\rho) + k_2 I_p \end{array}\right] \tag{46}$$

where k_2 is a fixed positive scalar. Substituting (46) into (43) and defining $\tilde{e}_{a_1}(t) := \mathrm{col}(d(t), \tilde{e}_1(t))$ yields

$$\underbrace{\left[\begin{array}{c} \dot{\tilde{e}}_{a_1}(t) \\ \dot{e}_y(t) \end{array}\right]}_{\dot{e}_a(t)} = \underbrace{\left[\begin{array}{cc} \tilde{A}_{a_{11}}(\rho) & 0 \\ \tilde{A}_{a_{21}}(\rho) & -k_2 I_p \end{array}\right]}_{\tilde{A}_o(\rho)} \underbrace{\left[\begin{array}{c} \tilde{e}_{a_1}(t) \\ e_y(t) \end{array}\right]}_{e_a(t)} - \underbrace{\left[\begin{array}{c} 0 \\ \tilde{F}_2 \end{array}\right]}_{\tilde{F}_a} f_\nu(t,\rho) + \underbrace{\left[\begin{array}{c} \tilde{M}_{a_1} \\ \tilde{M}_{a_2} \end{array}\right]}_{\tilde{M}_a} \xi_a(t) + \underbrace{\left[\begin{array}{c} 0 \\ I \end{array}\right]}_{\tilde{G}_{n_a}} \nu(t) \tag{47}$$

For the injection term $\nu(t) \in \mathbb{R}^p$, define the jth component as

$$\nu_j(t) = -k_1 \mathrm{sign}(e_{y,j}(t)) |e_{y,j}(t)|^{1/2} + z_j(t) \tag{48}$$

$$\dot{z}_j(t) = -k_3 \mathrm{sign}(e_{y,j}(t)) - k_4 e_{y,j}(t) \tag{49}$$

for $j = 1, 2, \ldots p$ where $e_y(t) = \mathrm{col}(e_{y,1}(t), e_{y,2}(t) \ldots e_{y,p}(t))$. The variables k_1, k_3, k_4 (and k_2) are design scalars to be chosen. The lower equations from (47) together with (48) can be written component-wise as

$$\dot{e}_{y,j}(t) = \tilde{\xi}_j(t) - k_2 e_{y,j}(t) - \tilde{F}_{2,j} f_\nu(t,\rho) + \nu_j(t) \tag{50}$$

where $\tilde{F}_{2,j}$ is the jth row of $\tilde{F}_2$ and

$$\tilde{\xi}_j(t) := \tilde{A}_{a_{21,j}}(\rho)\tilde{e}_{a_1}(t) + \tilde{M}_{a_2,j}\xi_a(t) \tag{51}$$

where $\tilde{A}_{a_{21,j}}(\rho)$ and $\tilde{M}_{a_2}$ the jth row of the matrices $\tilde{A}_{a_{21}}(\rho)$ and $\tilde{M}_{a_2}$ respectively. Consequently combining (48)-(50) yields

$$\begin{aligned} \dot{e}_{y,j}(t) &= -k_1\,\text{sign}(e_{y,j}(t))|e_{y,j}(t)|^{1/2} - k_2\,e_{y,j}(t) + z_j(t) + \tilde{\xi}_j(t) - \tilde{F}_{2,j}f_\nu(t,\rho) & (52)\\ \dot{z}_j(t) &= -k_3\,\text{sign}(e_{y,j}(t)) - k_4\,e_{y,j}(t) & (53)\end{aligned}$$

for $j = 1, 2, \ldots p$. Making the change of variable

$$\tilde{z}_j(t) := z_j(t) + \tilde{\xi}_j(t) - \tilde{F}_{2,j}f_\nu(t,\rho) \tag{54}$$

Equations (52)-(53) can be re-written as

$$\begin{aligned} \dot{e}_{y,j}(t) &= -k_1\,\text{sign}(e_{y,j}(t))|e_{y,j}(t)|^{1/2} - k_2\,e_{y,j}(t) + \tilde{z}_j(t) & (55)\\ \dot{\tilde{z}}_j(t) &= -k_3\,\text{sign}(e_{y,j}(t)) - k_4\,e_{y,j}(t) + \phi_i(t) & (56)\end{aligned}$$

where $\phi_i(t) = \dot{\tilde{\xi}}_j(t) - \tilde{F}_{2,j}\dot{f}_\nu(t,\rho)$, and furthermore

$$\begin{aligned} |\phi_i(t)| &< |\dot{\tilde{\xi}}_j(t)| + \|\tilde{F}_{2,j}\|\,\|\dot{f}_\nu(t,\rho)\| \\ &\leq \|\frac{\partial\tilde{A}_{21,j}}{\partial\rho}\|\,\|\dot{\rho}\|\,\|\tilde{e}_{a_1}(t)\| + \|\tilde{A}_{21,j}\|\,\|\dot{\tilde{e}}_{a_1}(t)\| + \|\tilde{M}_{a_2,j}\|\,\|\dot{\xi}_a\| + \|\tilde{F}_{2,j}\|\,\|\dot{f}_\nu(t,\rho)\| \end{aligned} \tag{57}$$

Since by assumption $\|\xi_a(t)\|$ is bounded and the autonomous system associated with the states $\tilde{e}_{a_1}(t)$ in (47) is stable, both $\|\tilde{e}_{a_1}(t)\|$ and $\|\dot{\tilde{e}}_{a_1}(t)\|$ are bounded. Provided $\|\dot{\rho}\|$ and $\|\dot{f}_\nu(t,\rho)\|$ are bounded, it follows $|\phi_i(t)| < \varepsilon$ for some sufficiently large scalar ε. Note that (55)-(56) is a special case of the super-twisting structure from [30]. As in [30] the gains from (55) and (56) are chosen as

$$\begin{aligned} k_1 &> 2\sqrt{\varepsilon} & (58)\\ k_2 &> 0 & (59)\\ k_3 &> \varepsilon & (60)\\ k_4 &> \frac{(k_2)^2\left((k_1)^3 + \frac{5}{4}(k_1)^2 + \frac{5}{2}(k_3-\varepsilon)\right)}{k_1(k_3-\varepsilon)} & (61)\end{aligned}$$

Consequently from the results in [30], it follows that $e_{y,j}(t) = \dot{e}_{y,j}(t) = 0$ in finite time. Therefore from (55), $\tilde{z}_j(t) = 0$ in finite time, and from the definition of the observer state $\tilde{z}_j(t)$ in (54) and the definition of $\nu_j(t)$ in (48)

$$\nu_j(t) := z_j(t) = \tilde{F}_{2,j}f_\nu(t,\rho) - \tilde{\xi}_j(t) \tag{62}$$

in finite time where $\tilde{\xi}_j(t)$ is defined in (51) and $\hat{f}_\nu(t,\rho) = WT^{\mathrm{T}}\nu_j(t) = f_\nu(t,\rho) - WT^{\mathrm{T}}\tilde{\xi}_j(t) = f_\nu(t,\rho) - G(s)\xi_a(t)$.

The virtual output fault $f_\nu(t,\rho)$ can be reconstructed online using (23) and $\nu(t)$ from (48). By assumption $E(\rho)$ is invertible, and therefore using the definition of $f_\nu(t,\rho)$ from (6), the real actuator fault can be estimated as

$$\hat{f}_i(t) = E(\rho)^{-1}\hat{f}_\nu(t,\rho) = E(\rho)^{-1}WT^{\mathrm{T}}\nu(t) \tag{63}$$

C. Design summary

This section will provide an over-view of the design process based on the exposition and developments in the previous section.

1) Recall, the objective is to synthesize the gains $G_l(\rho), G_n \in \mathbb{R}^{n\times p}$ for (8), and a scaling gain $\hat{W} \in \mathbb{R}^{q\times p}$ to create an observer of the form

$$\dot{\hat{x}}(t) = A(\rho)\hat{x}(t) + B(\rho)u(t) - G_l(\rho)e_y(t) + G_n\nu(t) \tag{64}$$

where in (64) the output error estimation signal is given by

$$e_y(t) = C\hat{x}(t) - y(t)$$

and the injection signal $\nu(t) \in \mathbb{R}^p$ is given componentwise by

$$\nu_j(t) \;=\; -k_1 \text{sign}(e_{y,j}(t))|e_{y,j}(t)|^{1/2} - \int_0^t (k_3 \text{sign}(e_{y,j}(s)) + k_4 e_{y,j}(s))\, ds \tag{65}$$

where $e_y(t) = \text{col}(e_{y,1}(t), e_{y,2}(t) \dots e_{y,p}(t))$. In (65) the variables k_1, k_3, k_4 are design scalars to be chosen. The fault reconstruction signal is then given by

$$\hat{f}(t) = \hat{W}\nu(t) \tag{66}$$

2) The fixed gain matrix G_n is parameterized by a matrix $L \in \mathbb{R}^{(n-p)\times p}$ in (15)-(16). The gain L is synthesized by solving an LMI optimization problem which minimizes the effect of uncertainty on the reconstruction signals given in (66). The user inputs to 'tune' the LMI solution are the design parameters

$$\Delta = \text{diag}(\delta_1, \delta_2) \tag{67}$$

where

$$\delta_1 = \text{diag}(\delta_{1,1} \dots \delta_{1,k}),\;\; \delta_2 = \text{diag}(\delta_{2,1} \dots \delta_{2,p})$$

which are used to trade-off the requirement for the fault estimation to be insensitive to uncertainty $\xi(t, y, u)$ in the plant in (1), and be insensitive to the imperfect measurements resulting from $\phi(t)$ in (4). The outputs of the LMI optimization associated with (34)-(35) are the gain matrix L and the reconstruction weighting matrix $\hat{W} \in \mathbb{R}^{q\times p}$ which is used in (66) to form the fault estimate.

3) Once L has been obtained, the gain G_n can be computed from (15).
4) Choose a design matrix of the form $-k_2 I_p$ where k_2 is a positive design scalar. This together with L parameterizes the varying gain $G_l(\rho)$ given in (46).
5) The scalar gains k_1, k_2, k_3, k_4 must be chosen to satisfy

$$k_1 > 2\sqrt{\varepsilon},\; k_2 > 0,\; k_3 > \varepsilon,\; k_4 > \frac{k_2^2\left(k_1^3 + \frac{5}{4}k_1^2 + \frac{5}{2}(k_3 - \varepsilon)\right)}{k_1(k_3 - \varepsilon)} \tag{68}$$

where ε is sufficiently large design scalar. This choice of scalars $k_1 \dots k_4$ will ensure a 2nd order sliding mode will take place in finite time, and be preserved in the face of faults, provide $|\dot{f}(t)| \le \varepsilon$.

IV. Sensor Fault Reconstruction

For a sensor fault reconstruction problem, consider an LPV plant represented by

$$\dot{x}(t) \;=\; A(\rho)x(t) + B(\rho)u(t) + M\xi(t, y, u) \tag{69}$$

$$y(t) \;=\; Cx(t) + Nf_o(t) + d(t) \tag{70}$$

The signal $f_o(t) \in \mathbb{R}^q$ is the (unknown) vector of sensor faults. Again $f_o \equiv 0$ represents fault–free conditions, while $f_o \neq 0$ indicates a fault exists in the sensors. Assume that

$$\|f_o(t)\| < a(t) \tag{71}$$

where $a(t) : \mathbb{R}_+ \mapsto \mathbb{R}^+$ is a known function. It is assumed that the columns of N are from the standard basis for $\mathbb{R}^p$, and the matrix N has full column rank. Again only the inputs $u(t)$ and the output measurements $y(t)$ are available for the FDI scheme. As before, the signal $d(t) \in \mathbb{R}^p$ represents a corruption of the true outputs and results in imperfect sensor measurements even in the fault free case where $f_o \equiv 0$. A clear distinction is therefore to be made between ever present (minor) corruption represented by $d(t)$ (noise perhaps) and infrequent but serious corruptions/biases/drifts etc represented by $f_o(t)$. Again it will be assumed that the signal $d(t)$ is low pass in terms of its frequency characteristics and satisfies (3).

By permutating the order of the outputs, without loss of generality, assume that the plant representation is in a form where the outputs which are prone to faults are in the lower half of the output equations, i.e.

$$y(t) = \begin{bmatrix} y_1(t) \\ \hline y_2(t) \end{bmatrix} \begin{matrix} \}\text{fault free} \\ \}\text{prone to fault} \end{matrix} = \underbrace{\begin{bmatrix} C_1 \\ \hline C_2 \end{bmatrix}}_{C} x(t) + \underbrace{\begin{bmatrix} 0 \\ \hline I_q \end{bmatrix}}_{N} f_o(t) + \underbrace{\begin{bmatrix} d_1(t) \\ \hline d_2(t) \end{bmatrix}}_{d} \tag{72}$$

where $C_1 \in \mathbb{R}^{(p-q)\times n}$ and $C_2 \in \mathbb{R}^{q\times n}$.

The idea is to re-formulate the sensor fault reconstruction problem as an actuator fault reconstruction scenario. This can be done by filtering the measured output $y_2(t)$ and augmenting it with the actual plant state $x(t)$. Consider the filtered output of $y_2(t)$ given by the state $z_f(t) \in \mathbb{R}^q$: specifically

$$\dot{z}_f(t) = -A_f z_f(t) + A_f y_2(t) \tag{73}$$

where $-A_f$ is a stable matrix belonging to $\mathbb{R}^{q\times q}$. Substituting $y_2(t)$ from (72) into (73) yields

$$\dot{z}_f(t) = -A_f z_f(t) + A_f C_2 x(t) + A_f f_o(t) + A_f d_2(t) \tag{74}$$

Next, augment system (69) and (74) to create a system of order $(n+q)$ of the form

$$\underbrace{\begin{bmatrix} \dot{x}(t) \\ \dot{z}_f(t) \end{bmatrix}}_{\dot{x}_s(t)} = \underbrace{\begin{bmatrix} A(\rho) & 0 \\ A_f C_2 & -A_f \end{bmatrix}}_{A_s(\rho)} \underbrace{\begin{bmatrix} x(t) \\ z_f(t) \end{bmatrix}}_{x_s(t)} + \underbrace{\begin{bmatrix} B(\rho) \\ 0 \end{bmatrix}}_{B_s(\rho)} u(t) + \underbrace{\begin{bmatrix} 0 \\ A_f \end{bmatrix}}_{F_s} f_o(t) + \underbrace{\begin{bmatrix} M & 0 \\ 0 & A_f \end{bmatrix}}_{M_s} \underbrace{\begin{bmatrix} \xi(t) \\ d_2(t) \end{bmatrix}}_{\xi_s(t)} \tag{75}$$

Replacing the system output $y_2(t)$ from (72), with the filtered version in (74), new 'outputs' (for the augmented system) can be represented by

$$\underbrace{\begin{bmatrix} y_1(t) \\ z_f(t) \end{bmatrix}}_{y_s(t)} = \underbrace{\begin{bmatrix} C_1 & 0 \\ 0 & I_q \end{bmatrix}}_{C_s} \underbrace{\begin{bmatrix} x(t) \\ z_f(t) \end{bmatrix}}_{x_s(t)} + \underbrace{\begin{bmatrix} d_1(t) \\ 0 \end{bmatrix}}_{d_s(t)} \tag{76}$$

Note that system (75) is in the form of an actuator fault reconstruction problem discussed in Section III and by construction rank$(C_s F_s) = q$ where C_s and F_s are defined in (76) and (75). The method described in the previous section can now be applied to the formulation in (75)-(76) to robustly estimate $f_o(t)$.

Remark: Note that augmenting the system in (69) with only the filtered faulty senors in (74) is different from the approach in [38] where the system is augmented with a filtered version of all the outputs of the plant[2] This is advantageous since the observer proposed here is lower order compared to the one in [38]. The choice of A_f does have a significant impact on the performance which can be achieved – particularly in terms of the $\mathcal{L}_2$ gain γ which is achieved. Here the emphasis is on achieving accuracy in terms of reconstructing the faults rather than accuracy of state estimation. The trade-off is explored and discussed in Section 8.5 of [4].

V. Sensor Fault Reconstruction Example

A. ADDSAFE Benchmark Design

The Advanced Fault Diagnosis for Sustainable Flight Guidance and Control (ADDSAFE) project is a European FP7 funded consortium which involves 8 partners (from 6 countries in Europe). The aim of ADDSAFE is to demonstrate the applicability of advanced fault detection and diagnosis (FDD) methods for aircraft, to support the development of sustainable aircraft. It addresses challenges to improve the FDD systems which support new 'green' technologies allowing optimization of the aircraft structural design, improving aircraft performance and reducing the environmental footprint [19].

One of the benchmark problems considered in ADDSAFE is a scenario involving a faulty yaw rate measurement. The sensor in the nonlinear ADDSAFE model has triple redundancy, and the actual measurement used for the controller calculations is decided by a consistency check (vote) between the three sensors measurements [18]. The detection and isolation of a faulty yaw rate sensor is one scenario which will be investigated in the ADDSAFE project and constitutes one of the benchmark problems to be tackled by the consortia.

The LPV plant used in the design presented in this paper is a lateral model obtained from [39], [23]. The model is derived from the ADDSAFE benchmark model using an LPV generation procedure described in [32]. The method involves the generation of a set of linearized models at equilibrium/trim points which are enclosed within the range of the LPV parameters. The elements of all the state space matrices are generated from a polynomial fit using least squares. The resulting polynomials can be used to create a single LPV model which approximates the whole set of

[2]It should be noted that the conceit of 'converting' a sensor fault problem into an actuator fault scenario for the purpose of developing an FDI scheme is not uncommon in the literature – see for example [35], [27].

number	axis	control surface
$1-2$	longitudinal	engine(PLA) $[pi_1\ pi_2]$
$3-4$	longitudinal	elevators $[profD\ ProfG]$
5	longitudinal	stabilizer $[ih]$
6	lateral	rudder
$7-10$	lateral	ailerons $[AilIntG\ AilIntD\ AilExtG\ AilExtD]$
$11-18$	lateral	spoilers $[Sp1G\ Sp1D\ Sp23G\ Sp23D\ Sp45G\ Sp45D\ Sp6G\ Sp6D\ ]$

TABLE I
CONTROL SURFACES

LTI equilibrium models [39], [23]. Further details of the LPV model and its generation are available in [39], [23], [32].

In [39], [23] the LPV parameters ρ, chosen to describe the variation of the aircraft dynamics, are mass (m), center of gravity in the x-direction (X_{cg}), altitude (h), and conventional airspeed (V_{cas}). The LPV model is valid for variations of $\pm 10\%$ for mass (m) and position of center of gravity (X_{cg}) as a percentage of the mean aerodynamic chord (mac), $\pm 25\%$ for altitude (h) and $\pm 19\%$ for conventional airspeed (V_{cas}) from the trim point

$$[m(0)\ X_{cg}(0)\ h(0)\ V_{cas}(0)]^{\mathrm{T}} = [200,000(kg)\ 30\%(\text{mac})\ 20,000(ft)\ 290(kt)]^{\mathrm{T}}$$

The states, outputs and control surface deflections for the LPV model are given in (77), (78) and Table I.

$$x_{LPV} = [\theta(rad),\ V_x(m/s),\ V_z(m/s),\ q(rad/s),\ h\ (m),\ \phi(rad),\ V_y(m/s),\ p(rad/s),\ r(rad/s)]^{\mathrm{T}} \quad (77)$$

$$y_{LPV} = [\theta(deg),\ \phi(deg),\ \alpha_{air}(deg),\ \beta(deg),\ p(deg/s),\ q(deg/s),\ r(deg/s),\ n_z,\ V_{tas}(kt)]^{\mathrm{T}} \quad (78)$$

For the design which will be presented in this paper, only the lateral model will be considered consisting of the states

$$x = [\phi\ V_y\ p\ r]^{\mathrm{T}}$$

The lateral control surfaces are rudder, ailerons and spoilers (13 surfaces). Note that since $V_y(t)$ is not one of the measured outputs of the aircraft and in order to obtain a fixed output distribution matrix C (as in equation (70)), $V_y(t)$ is approximated in real-time from the measurements of $\beta(t)$ and $V_{tas}(t)$ via the equation

$$V_y(t) = V_{tas}(t)\ \sin(\beta(t)) \quad (79)$$

This approximation is achieved through the transformation from flight path axis to body axis [33].
The LPV system matrices are given by

$$A(\rho) = A_0 + A_1\rho_1 + A_2\rho_2 + A_2\rho_2 + A_3\rho_3 + A_4\rho_4 \quad (80)$$

$$B(\rho) = B_0 + B_1\rho_1 + B_2\rho_2 + B_2\rho_2 + B_3\rho_3 + B_4\rho_4 \quad (81)$$

where

$$[\rho_1, \rho_2, \rho_3, \rho_4] := [\bar{m}, \bar{X}_{cg}, \bar{h}, \bar{V}_{cas}] \quad (82)$$

represent normalized parameters varying in the interval $[-1\ 1]$. The normalized parameters are given by

$$\bar{m} = \frac{m - 200000}{20000},\ \bar{X}_{cg} = \frac{X_{cg} - 0.3}{0.03},\ \bar{h} = \frac{h - 20000}{5000},\ \bar{V}_{cas} = \frac{V_{cas} - 290}{30} \quad (83)$$

where $m,\ X_{cg},\ h,\ V_{cas}$ vary in the range of $m(kg) \in [180,000\ 220,000]$, $X_{cg} \in [0.27\ 0.33]$, $h(ft) \in [15,000\ 25,000]$ and $V_{cas}(kt) \in [260\ 320]$ respectively.

One of the scenarios considered in the ADDSAFE benchmark problem involves a faulty yaw rate $r(t)$ sensor. Therefore the original lateral states of the LPV model $x = [\phi\ V_y\ p\ r]^{\mathrm{T}}$ are already in the canonical form in (72)

where the sensor prone to faults $r(t)$ is at the bottom of the output vector: specifically

$$\begin{aligned} x(t) &= y(t) = \left[\begin{array}{c} y_1(t) \\ \hline y_2(t) \end{array}\right] = \left[\begin{array}{c} \phi(t) \\ V_y(t) \\ p(t) \\ \hline r(t) \end{array}\right] \begin{array}{l} \Big\} \text{fault free} \\ \Big\} \text{prone to fault} \end{array} \\ &= \begin{array}{l} C_1\{ \\ C_2\{ \end{array} \underbrace{\left[\begin{array}{cccc} 1 & 0 & 0 & 0 \\ 0 & 1 & 0 & 0 \\ 0 & 0 & 1 & 0 \\ \hline 0 & 0 & 0 & 1 \end{array}\right]}_{C} x(t) + \underbrace{\left[\begin{array}{c} 0 \\ 0 \\ 0 \\ \hline 1 \end{array}\right]}_{N} F_o(t) + \begin{array}{l} d_1\{ \\ d_2\{ \end{array} \underbrace{\left[\begin{array}{c} d_{11}(t) \\ d_{12}(t) \\ d_{13}(t) \\ \hline d_2(t) \end{array}\right]}_{d(t)} \end{aligned}$$

Here $n = 4, p = 4, q = 1$. The scalar variable A_f (in this case) which defines the output filter in (73), has been chosen as $A_f = 1$. The fixed component of the augmented system in (75) is $A_f C_2 = \left[\begin{array}{cccc} 0 & 0 & 0 & 1 \end{array}\right]$. The new augmented system output in (76) is

$$\underbrace{\left[\begin{array}{c} y_1(t) \\ z_f(t) \end{array}\right]}_{y_s} = \underbrace{\left[\begin{array}{ccccc} 1 & 0 & 0 & 0 & 0 \\ 0 & 1 & 0 & 0 & 0 \\ 0 & 0 & 1 & 0 & 0 \\ \hline 0 & 0 & 0 & 0 & 1 \end{array}\right]}_{C_s} \underbrace{\left[\begin{array}{c} x(t) \\ z_f(t) \end{array}\right]}_{x_s} \tag{84}$$

where y_s and x_s are in the coordinates defined in (75). Permutating the states $x_s(t)$ from (84) into

$$\left[\begin{array}{c|cccc} r(t) & \phi(t) & V_y(t) & p(t) & z_f(t) \end{array}\right]^{\mathrm{T}} = \left[\begin{array}{c} x_1(t) \\ x_2(t) \end{array}\right] \tag{85}$$

bring about the canonical form in (13)-(14) where $C = \left[\begin{array}{cc} 0 & I_4 \end{array}\right]$ and $F = \left[\begin{array}{cc} 0_{1\times 4} & 1 \end{array}\right]^{\mathrm{T}}$. It is assumed that the uncertainty is dominant in the roll rate and yaw rate channels and therefore the uncertainty matrix from (69) is given by

$$M = \left[\begin{array}{ccccc} 1 & 0 & 0 & 0 & 0 \\ 0 & 0 & 0 & 1 & 0 \end{array}\right]^{\mathrm{T}} \tag{86}$$

The design scalar a_f from (4) has been chosen as $a_f = 25$. It is assumed that the effect of uncertainty is small compared to the effect of 'sensor noise'. In this particular design $\delta_1 = 0.0001 I_2$. Here, other than the fault f_o, it is assumed that there is no corruption to the state z_f i.e. $d_2(t) = 0$ in $\xi(t)$ from (75) and the parameter δ_2 has been chosen as $\delta_2 = diag(1, 60, 1, 0)$. Note that the second parameter in δ_2 corresponds to V_y which has magnitude (unit kt) larger than the rest of the states (unit rad) and is therefore weighted more heavily. The last parameter in δ_2 corresponds to the zero in $d(t)$ from (76). Using the above parameters in the LMIs in (34)-(35), yields $L = [0.1848 \ 0.0048 \ -0.0000 \ 0]$ from (16). The gains for the 'output injection signal' in (52)-(53) have been chosen as $k_1 = 2.1, k_2 = 0.32, k_3 = 2, k_4 = 0.9853$.

B. ADDSAFE Simulation Results

Several flight conditions and manoeuvres have been tested to assess the performance of the proposed scheme. The results presented below show some of the simulation results which have been obtained. A few initial conditions will be considered to cover all the extremes of the LPV parameter range to highlight the potential of the proposed scheme to cover a wide range of operating conditions.

Note that although the observer design is based on an LPV system, the results presented in this paper are based *on the full nonlinear model of the aircraft*. Realistic sensor and actuator dynamics as well as noise have been included in the simulation [20], [19]. Also note that during the simulation, the mass and center of gravity do not change significantly and therefore are not plotted.

Remark: Due to industrial confidentiality constraints, the results in the subsequent figures are expressed in terms of percentage of the admissible range.

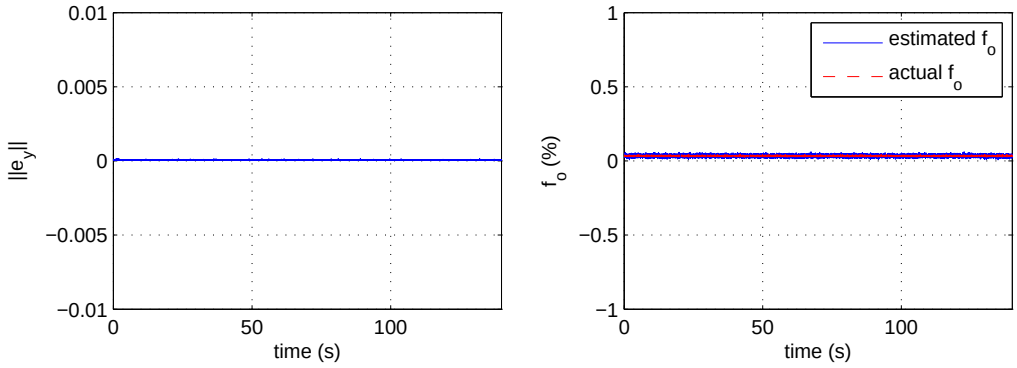

(a) fault free: observer errors & fault reconstructions

Fig. 1. At Trim - Straight and Level Flight: Fault Free

1) At Trim - Straight and Level Flight: This simulation was conducted using an initial condition $[m,\ X_{cg},\ h,\ V_{cas}] = [200000kg,\ 30\%,\ 20000ft,\ 290kt]$. The aircraft is initially on a straight and level flight path.

Fault Free: Figure 1 shows the results from a fault free condition. Here the unmeasured state $V_y(t)$ has been estimated as in (79) which enables $V_y(t)$ to be used by the observer scheme. Figure 1(a) shows the magnitude of the observer error signals combined and represented as a norm. This signal is small and therefore indicates that a sliding motion is occurring. Figure 1(a) also shows the reconstructed sensor fault signals, where as expected, for a fault free case, are close to zero.

Additive Fault: Figure 2 shows the result of an additive fault on the yaw rate sensor. Figure 2(a) shows the effect of a sensor fault on the closed loop aircraft behaviour. Here the aircraft roll becomes nonzero causing a nonzero yaw and generating a side force. Figure 2(b) shows the additive fault appears at 10sec and the faulty measurement causes degradation in the closed loop performance as shown in Figure 2(a). Figure 2(c) shows the changes to the LPV parameters V_{cas} and h. Figure 2(d) shows that sliding still occurs as $\|e_y\|$ is close to zero. This figure also shows that the fault occurs at 10sec and the reconstruction of the fault provides a good estimate of the actual additive fault (both lines overlap).

Figure 3 shows the performance of the reconstruction scheme on both the full nonlinear plant, and also when applied to the plant when represented by the LPV model (about which the observer is designed). As expected the reconstruction is perfect when used with the LPV plant subject to the additive fault, whereas, whilst the reconstruction obtained for the nonlinear plant is excellent, it is no longer perfect because of the plant/model mismatch.

2) Low End of the LPV Range - Straight and Level Flight: This simulation was conducted using an initial condition $[m,\ X_{cg},\ h,\ V_{cas}] = [185000kg,\ 28\%,\ 17000ft,\ 267kt]$ based on a straight and level flight. This initial condition is at the low end of the LPV parameter range.

NRZ: Figure 4 shows the results for the case when the sensor output is subjected to a no-return-to-zero (NRZ) fault. Again for this fault case, a 'zoomed in plot' is considered. Figure 4(b) shows the fault in comparison with the actual yaw rate (which has become nonzero due to the degradation in performance resulting from the faulty measurement used by the controller). Figure 4(d) shows that sliding occurs and the faults have been reconstructed with satisfactory accuracy.

3) High End of the LPV Range - Coordinated Turn: This simulation was conducted using an initial condition $[m,\ X_{cg},\ h,\ V_{cas}] = [210000kg,\ 32\%,\ 23000ft,\ 300kt]$ with a coordinated turn which starts at 10sec and ends at 30 sec. This choice of initial condition is at the high end of the LPV parameter range.

Fast Runaway: Figure 5 shows the results when the yaw rate sensors have a fast runaway. Figure 5(a) shows that after 10sec a roll to the left starts to allow for a left turn and at 20sec the fast runaway starts to develop (Figure 5(b)). Once the faults have occurred, the controller performance degrades (as shown in 5(a)) and the aircraft does not return to level flight after 30sec. Figure 5(c) shows a large variation in speed and altitude due to the degradation in the controller performance resulting from the faulty measurement. These changes also highlight the ability of the observer model to handle variations in the operating condition and allows a sliding motion to be maintained. Accurate fault reconstruction is achieved as shown in 5(d).

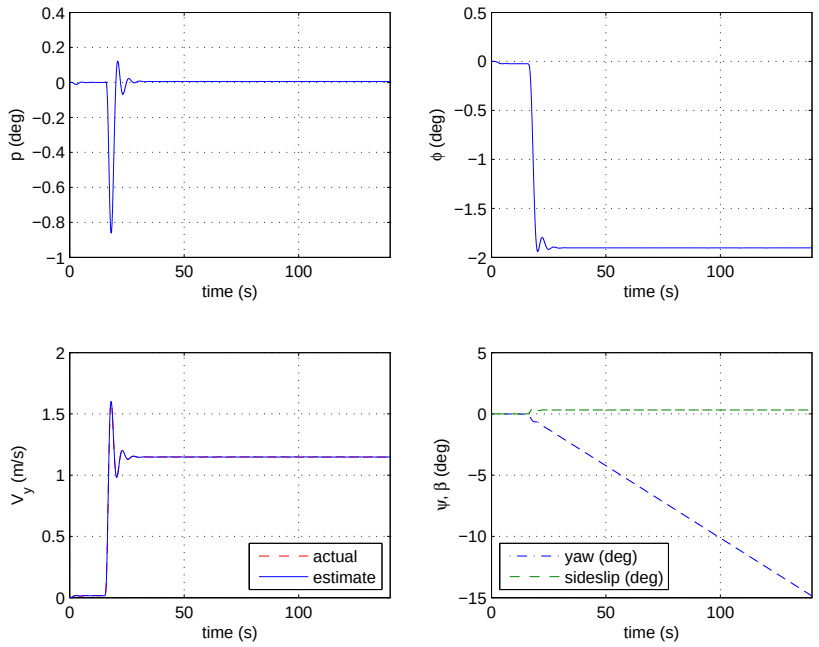

(a) additive fault: states $x(t)$

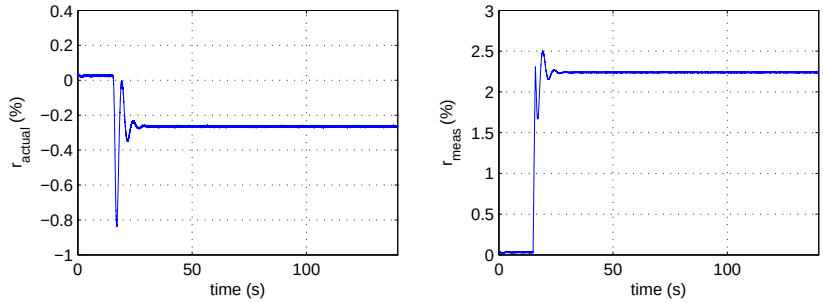

(b) additive fault: $r(t)$

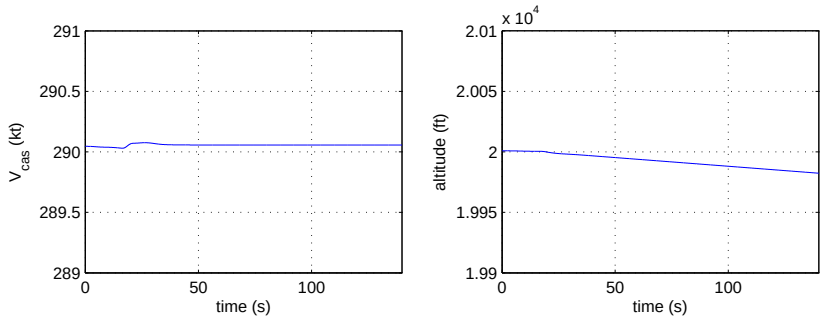

(c) additive fault: LPV parameter ρ

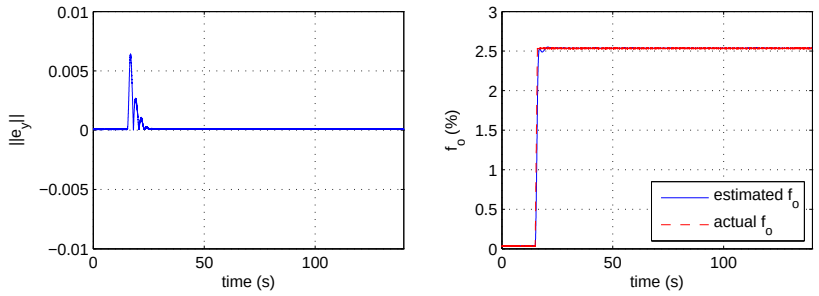

(d) additive fault: observer errors & fault reconstructions

Fig. 2. At Trim - Straight and Level Flight: Additive Fault

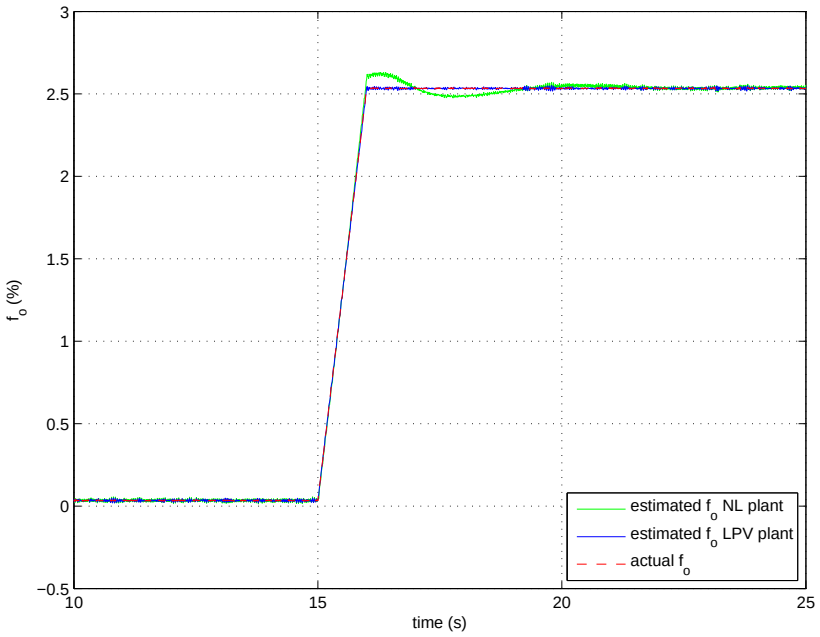

Fig. 3. Comparison of the reconstruction from the nonlinear plant and the approximate LPV plant model

VI. Conclusions

This paper has presented a robust fault reconstruction method for LPV systems based on sliding mode observers where both actuator and sensor faults have been considered. The observer is designed using LMIs to minimize the effect of uncertainty and measurement corruptions on the fault reconstruction. For actuator fault reconstruction, the varying input distribution matrix (associated with the monitored channels) is factorized into fixed and varying parts. The observer is then designed based on the resulting virtual system. In the observer, the gain associated with the nonlinear injection term is fixed, while the gain associated with the linear injection is varying. The faults associated with the virtual system are reconstructed using the equivalent output error injection signal and are mapped back into actual faults by considering the factorization of the input distribution matrix. The output error injection signal is supplied by a second order sliding mode scheme which does not require any 'smoothing' and therefore provides an ideal sliding motion. A rigorous stability analysis and the existence of a sliding motion has also been presented. For sensor fault reconstruction, the idea is to convert the sensor fault reconstruction problem into an actuator scenario so that the same design procedure applies. This conversion is achieved by augmenting the plant states with the filtered output measurements which are prone to faults. This augmentation is different compared to other schemes previously considered in the literature (where the plant states are augmented with the filtered output of all the output measurements). Simulations using a full nonlinear model of a large transport aircraft associated with the ADDSAFE project have been presented. The sensor fault reconstructions presented here are from a benchmark problem under investigation in the ADDSAFE project and represent a realistic industrial problem. The results consider several manoeuvres and flight conditions to highlight the ability of the proposed scheme to reconstruct faults for a wide range of operating conditions. All the results have shown good reconstruction performance highlighting the potential of the proposed scheme.

References

[1] M. O. Abdalla, E. G. Nobrega, and K. M. Grigoriadis. Fault detection and isolation filter design for linear parameter varying systems. In *Proceedings of the American Control Conference*, pages 3890 – 3895, 2001.

[2] H. Alwi and C. Edwards. Fault detection and fault-tolerant control of a civil aircraft using a sliding-mode-based scheme. *IEEE Transactions on Control Systems Technology*, 16(3):499–510, 2008.

[3] H. Alwi, C. Edwards, and A. Marcos. Fault Reconstruction Using a LPV Sliding Mode Observer for a Class of LPV Systems. *Journal of The Franklin Institute*, 349(2):510–530, 2012.

[4] H. Alwi, C. Edwards, and C.P. Tan. Fault Detection and Fault-Tolerant Control Using Sliding Modes. AIC, Springer Verlag, 2011.

[5] F. Amato, M. Mattei, R. Iervolino, and G. Paviglianiti. A nonlinear UIO scheme for the FDI on a small commercial aircraft. In *IEEE International Conference on Control Applications*, pages 235–240, 2002.

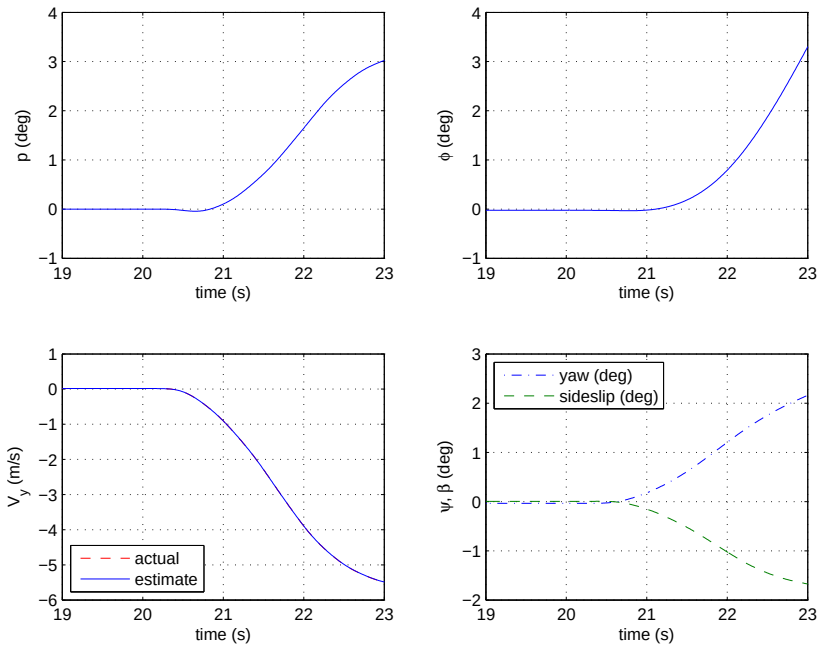

(a) NRZ: states $x(t)$

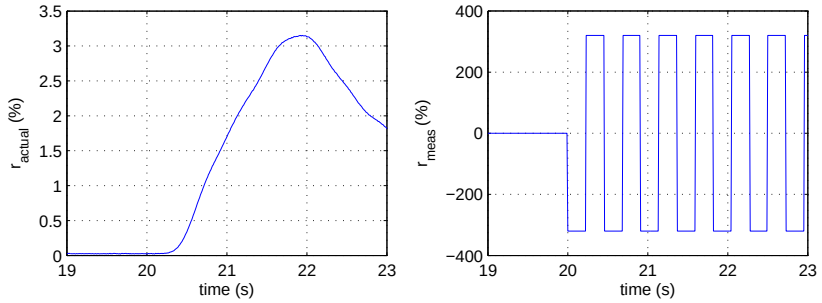

(b) NRZ: states $r(t)$

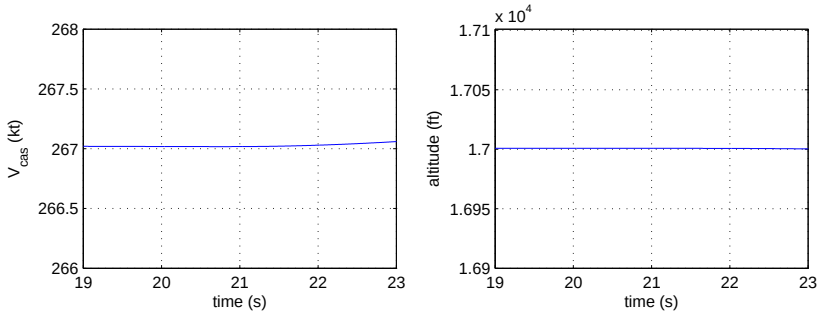

(c) NRZ: LPV parameter ρ

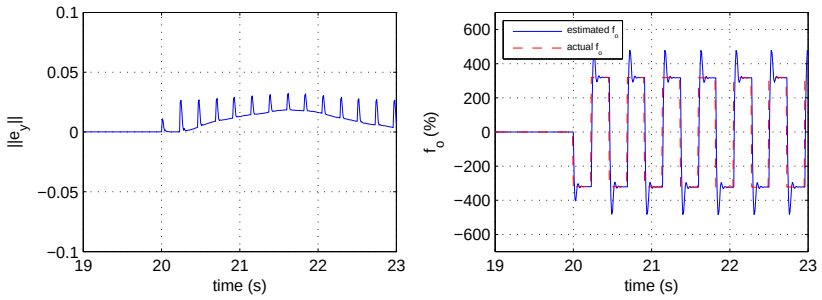

(d) NRZ: observer errors & fault reconstructions

Fig. 4. Low End of LPV Range - Straight and Level Flight (zoomed): NRZ fault

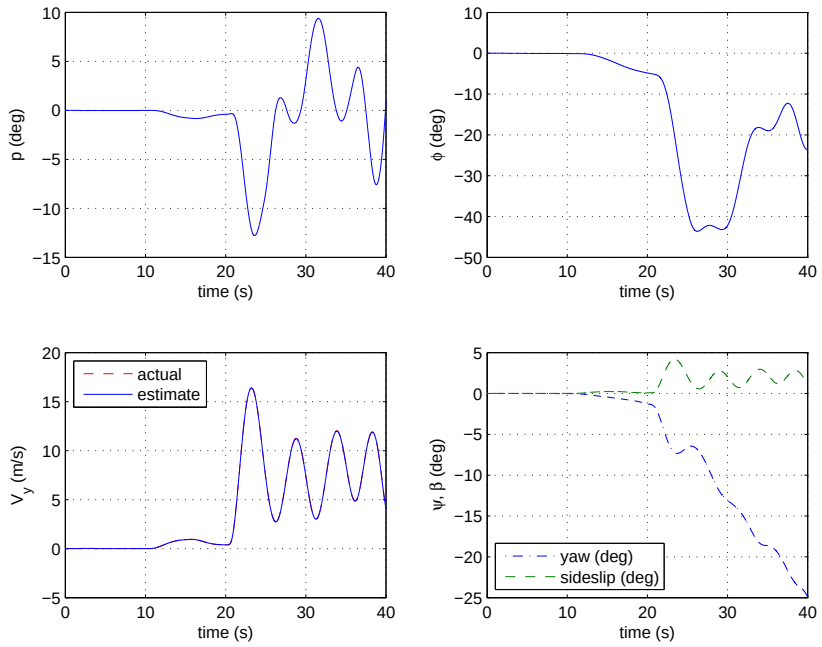

(a) fast runaway: states $x(t)$

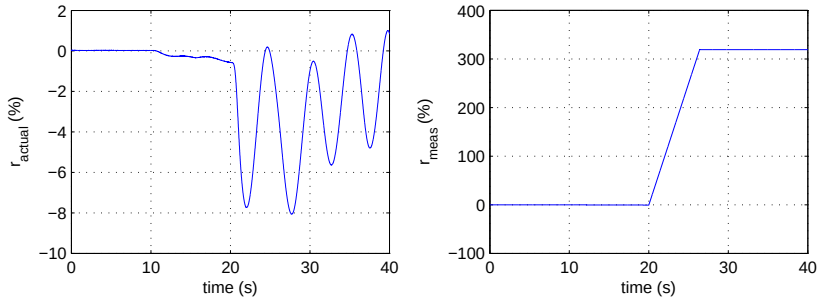

(b) fast runaway: $r(t)$

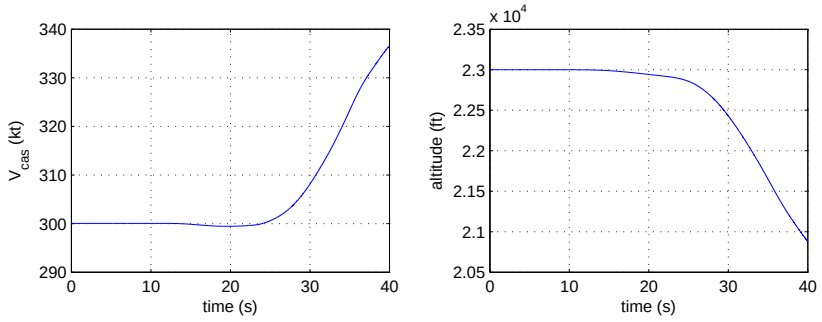

(c) fast runaway: LPV parameter ρ

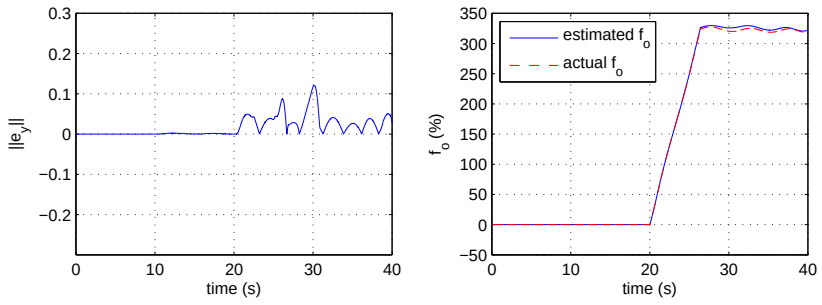

(d) fast runaway: observer errors & fault reconstructions

Fig. 5. High End of LPV Range - coordinated turn: fast runaway fault

[6] P. Apkarian, P. Gahinets, and G. Becker. Self-scheduled $\mathcal{H}_\infty$ control of linear parameter-varying systems: a design example. *Automatica*, 31(9):1251–1261, 1995.

[7] S. Armeni, A. Casavola, and E. Mosca. Robust fault detection and isolation for LPV systems under a sensitivity constraint. *International Journal Of Adaptive Control And Signal Processing*, 23:55–72, 2009.

[8] G. J. Balas. Linear, parameter–varying control and its application to a turbofan engine. *International Journal of Robust and Nonlinear Control*, 12:763–796, 2002.

[9] J. Bokor and G.J. Balas. Detection filter design for LPV systems - a geometric approach. *Automatica*, 40:511–518, 2004.

[10] J. Bokor, Z. Szabo, and G. Stikkel. Failure detection for quasi LPV systems. In *IEEE Conf. on Decision and Control*, 2002.

[11] A. Casavola, D. Famularo, G. Franz, and M. Sorbara. A fault-detection, filter-design method for linear parameter-varying systems. *Proceedings of the Institution of Mechanical Engineers, Part I: Journal of Systems and Control Engineering*, 221(6):865–874, 2007.

[12] P. Castaldi, W. Geri, M. Bonfé, S. Simani, and M. Benini. Design of residual generators and adaptive filters for the FDI of aircraft model sensors. *Control Engineering Practice*, 18(5):449–459, 2010.

[13] C. Edwards and S. K. Spurgeon. *Sliding Mode Control: Theory and Applications*. Taylor & Francis, 1998.

[14] C. Edwards, S.K. Spurgeon, and R.J. Patton. Sliding mode observers for fault detection. *Automatica*, 36:541–553, 2000.

[15] D. Efimov, L. Fridman, T. Raissi, A. Zholgadri and R. Eydou. Interval estimation for LPV systems applying higher order sliding mode techniques *Automatica*, 48:2365–2371, 2012.

[16] L. Fridman, Y. Shtessel, C. Edwards, and X.G. Yan. Higher-order sliding-mode observer for state estimation and input reconstruction in nonlinear systems. *International Journal of Robust and Nonlinear Control*, 18(4-5):399412, 2008.

[17] P. Gahinet, A. Nemirovski, A. Laub, and M. Chilali. *LMI Control Toolbox, User Guide*. MathWorks, Inc., 1995.

[18] P. Goupil. AIRBUS state of the art and practices on FDI and FTC in flight control system. *Control Engineering Practice*, 19(6):524–539, 2011.

[19] P. Goupil and A. Marcos. Advanced Diagnosis for Sustainable Flight Guidance and Control: The European ADDSAFE Project. In *SAE AeroTech Congress & Exhibition*, 2011.

[20] P. Goupil and G. Puyou. A high fidelity AIRBUS benchmark for system fault detection and isolation and flight control law clearance. In *European Conference for AeroSpace Sciences (EUCASS'11)*, 2011.

[21] S. Grenaille, D. Henry, and A. Zolghadri. A method for designing fault diagnosis filters for LPV polytopic systems. *Journal of Control Science and Engineering*, 2008.

[22] R. Hallouzi, V. Verdult, R. Babuska, and M. Verhaegen. Fault detection and identification of actuator faults using linear parameter varying models. In *Preprints of the IFAC World Congress*, 2005.

[23] S. Hecker. Nominal and faulty LFT/LPV models. ADDSAFE report D1.3.2-3, DLR, 2010.

[24] F.J.J. Hermans and M.B. Zarrop. Sliding mode observers for robust sensor monitoring. In *Proceedings of the 13th IFAC World Congress*, pages 211–216, 1996.

[25] T. H. Khong and J. Shin. Robustness analysis of integrated LPV-FDI filters and LTI-FTC system for a transport aircraft. In *AIAA Guidance, Navigation and Control Conference and Exhibit*, number AIAA 2007-6771, 2007.

[26] Y. W. Kim, G. Rizzoni, and V. Utkin. Developing a fault tolerant power train system by integrating the design of control and diagnostics. *International Journal of Robust and Nonlinear Control*, 11:1095–1114, 2001.

[27] M.A. Massoumnia, G.C. Vergese, and A.S. Willsky. Fault detection and identification. *IEEE Transactions on Automatic Control*, 34:316–321, 1989.

[28] A. Marcos and G. J. Balas. A Boeing 747–100/200 aircraft fault tolerant and diagnostic benchmark. Technical Report AEM–UoM–2003–1, Department of Aerospace and Engineering Mechanics, University of Minnesota, 2003.

[29] A. Marcos and G. J. Balas. Development of linear-parameter-varying models for aircraft. *AIAA Journal of Guidance, Control and Dynamics*, 27(2):218–228, 2004.

[30] J.A. Moreno and Marisol Osorio. Strict lyapunov functions for the super-twisting algorithm. *IEEE Transactions on Automatic Control*, 57(4):1035–1040, 2012.

[31] K. Nonami and S. Sivrioglu. Sliding mode control with gain scheduled hyperplane for LPV plant. In K. D. Young and Ü. Özgüner, editors, *Variable structure systems, sliding mode and nonlinear control*, pages 263–279. Springer Verlag, 1999.

[32] H. Pfifer and S. Hecker. Generation of optimal linear parametric models for LFT-based robust stability analysis and control design. In *Proceedings of the 47th IEEE Conference on Decision and Control, CDC*, pages 3866–3871, 2008.

[33] M. O. Rauw. *FDC 1.2 - A Simulink Toolbox for Flight Dynamics and Control Analysis*. Haarlem, The Netherlands, 2001.

[34] M. Sato. Filter design for LPV systems using quadratically parameter-dependent lyapunov functions. *Automatica*, 42(11):2017–2023, 2006.

[35] M. Saif and Y. Guan. A new approach to robust fault detection and identification. *IEEE Transactions on Aerospace and Electronic Systems*, 29:685–695, 1993.

[36] S. Sivrioglu and K. Nonami. Sliding mode control with time-varying hyperplane for AMB systems. *IEEE/ASME Transactions On Mechatronics*, 3(1):51–59, 1998.

[37] I. Szaszi, A. Marcos, G. J. Balas, and J. Bokor. Linear parameter-varying detection filter design for a Boeing 747-100/200 aircraft. *Journal of Guidance, Control, and Dynamics*, 28(3):461–470, 2005.

[38] C. P. Tan and C. Edwards. Sliding mode observers for robust detection and reconstruction of actuator and sensor faults. *International Journal of Robust and Nonlinear Control*, 13:443–463, 2003.

[39] A. Varga, S. Hecker, and D. Ossmann. Diagnosis of actuator faults using LPV-gain scheduling techniques. In *AIAA Guidance, Navigation and Control Conference and Exhibit*, number AIAA-2011-6680, 2011.

[40] M. Verhaegen, S. Kanev, R. Hallouzi, C. Jones, J. Maciejowski, and H. Smail. Fault tolerant flight control - a survey. In C. Edwards, T. Lombaerts, and H. Smaili, editors, *Fault Tolerant Flight Control*, pages 47–89. Springer Verlag, 2010.

[41] X. Wei and M. Verhaegen. Mixed $\mathcal{H}_-/\mathcal{H}_\infty$ fault detection observer design for LPV systems. In *IEEE Conference on Decision and Control*, pages 1073–1078, 2008.

[42] X. G. Yan and C. Edwards. Nonlinear robust fault reconstruction and estimation using a sliding mode observer. *Automatica*, 43(9):1605–1614, 2007.

[43] H. Yang and M. Saif. Fault detection in a class of nonlinear systems via adaptive sliding observer. In *Proceedings of the IEEE International Conference on Systems, Man and Cybernetics*, pages 2199–2204, 1995.

[44] Y. M. Zhang and J. Jiang. Active fault-tolerant control system against partial actuator failures. *IEE Proceedings: Control Theory & Applications*, 149:95–104, 2002.